Initial Results of Elemental Composition Analysis Using NRTA With An Isotopic Neutron Source

Farheen Naqvi,* Peninah Levine, Ethan A. Klein, and Areg Danagoulian
Department of Nuclear Science and Engineering, MIT, Cambridge, MA 02139, USA
(Dated: August 5, 2021)

I. ABSTRACT

Neutron resonance transmission analysis technique (NRTA) uses the resonance phenomenon to identify the isotopic composition of unknown materials. Several mid-Z to high-Z elements have discrete energy levels $1-100$ eV above the neutron separation energy. In this energy range, the transmission spectra of epithermal neutrons for these elements show unique resonant signatures due to which NRTA has found its applications in the field of archaeology, warhead verification and spent fuel analysis. Presence and quantification of special nuclear materials such as U-235, U-238, Pu-239 and Pu-240 with NRTA is being explored, however its application is still limited due to the availability of calibrated, strong neutron sources only at large experimental facilities. To eliminate this limitation, we have studied the feasibility of doing NRTA with a mobile, small-scale setup using an isotopic neutron source. Time-of-flight is measured between two detectors to provide energy of the transmitted epithermal neutrons. One of the detectors also acts as moderator to produce epithermal neutrons. Proposed experimental geometry, measurements times and acceptable source rates investigated using Monte Carlo based GEANT4 code are presented in this report. These results constitute a test of feasibility, and will inform future experimental measurements.

II. INTRODUCTION

Neutron Resonance Transmission Technique (NRTA) is an established method for identifying the elemental and isotopic composition of samples [1–11]. Every isotope has a unique reaction cross-section dependence on the energy of incoming neutrons. An enhancement in the reaction cross section at neutron energies corresponding to the nuclear excited state energies gives rise to resonances. In the energy range of $1-100$ eV the total cross section is dominated by resonant reactions such as elastic scattering, absorption or fission. The observed resonances are narrow and discrete for most of the commonly encountered isotopes especially U-235, U-238, Pu-239 and Pu-240 that are of interest for nuclear security and safeguards [12]. The NRTA technique exploits this resonance phenomenon by identifying the attenuation dips in the neutron transmission spectrum through an unknown target and uniquely associating them with the individual isotopes present within.

Though the observed attenuation dips in the neutron transmission spectrum are well separated, to unambiguously identify multiple elements in a target with small cross sections, it is important to have a setup with good spectral resolution. Due to this requirement, in the past, NRTA was only done at experimental facilities measuring neutron time-of-flight in long beam lines using pulsed and high-flux neutron sources, thereby limiting the technique's potential applications. Recent work has focused on reducing the footprint of the experimental setup by employing small accelerators for neutron production [13]. On the same line of thought, a recent study has demonstrated the possibility of using a compact and portable NRTA experimental setup with Deuterium-Tritium neutron generator to provide isotopic identification of several mid-Z elements [14]. Such an approach would open avenues for an on-site material investigation essential for nuclear security.

In this work we are exploring an additional approach which forgoes a pulsed source altogether and instead uses an isotopic neutron source such as americium beryllium (AmBe) or plutonium beryllium (PuBe). This would make

* fnaqvi@mit.edu

the experimental setup even more compact and mobile. In other NRTA experiments a pulsed beam is required for providing a time reference to calculate the time-of-flight of neutrons. Instead, the setup proposed in this study uses an active moderator-detector for providing the start (T_0) signal. A plastic or EJ-309 liquid scintillator detector acts as a moderator with hydrogenous material to reduce the energy of the neutrons emitted while also providing the time information of neutron interactions. Since (T_0) is the time of the first elastic interaction of the neutron in moderation process and is taken from a fast plastic scintillator, the time resolution of the setup is no longer limited by the pulse width, it rather is a function of variation in time required by the neutrons to get moderated to $\sim$ eV energy. This approach requires an optimization of the moderator dimensions, detector shielding and source rates to maximize the epithermal neutron output and minimize the background. To achieve this, Monte Carlo (MC) simulations using GEANT4 based grasshopper software [15] were performed and a careful investigation of moderator assembly in combination with detector placement with different source activity was done.

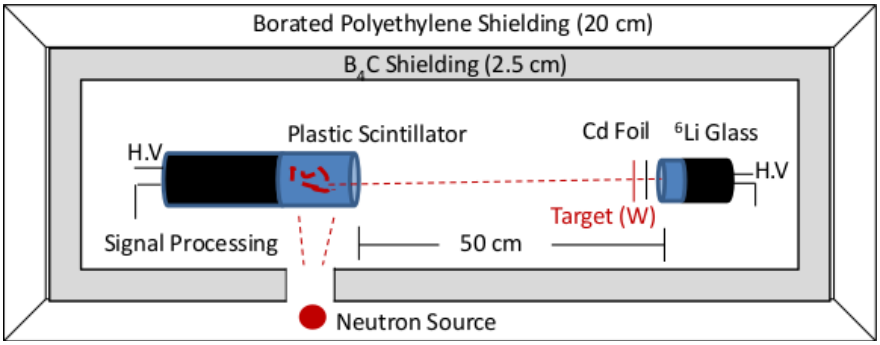

FIG. 1. Schematic of the experimental setup. The AmBe neutron source is embedded in a layer of 20-cm thick borated polyethylene followed by a 2.5-cm thick B_4C layer. The fast neutrons are incident on a plastic scintillator also used as a moderator to reduce the energy of the neutrons. Moderated beam is incident on a target and detected in a 1-cm thick ^{6}Li-enriched GS20 glass scintillator coupled to a photomultiplier tube. The detector is shielded from off-axis epithermal neutrons by boron carbide. Thermal neutrons are filtered by 3.0 mm of cadmium foil placed in front of the detector collimator geometry. Time-of-flight is measured between the plastic scintillator and GS20 glass detector.

III. MONTE CARLO SIMULATIONS

A. Proposed Experimental Setup

A complete schematic diagram of the simulated experimental setup is shown in Fig. 1. Neutron beam was generated by an AmBe source emitting $\sim 10^4$ neutrons per second. Higher source rates were also considered to understand the background contributions. A detailed discussion on this topic is given in III C. Neutrons were emitted isotropically and the ISO 8529 energy distribution characteristic of AmBe emission was taken from Ref. [16]. For moderating the emitted neutrons to the epithermal energy range, a cylindrical plastic scintillator was placed $\sim$ 5cm away from the AmBe source. The resulting epithermal neutrons were detected in a 1 cm-thick, 15 cm-wide ^{6}Li-enriched GS20 glass detector placed 50 cm away from the face of the plastic scintillator. Coincident events between the two detectors yielded time-of-flight (TOF) information of the neutrons. For a defined TOF distance, d_{TOF}, the following non-relativistic relationship was used to determine the neutron energy, E_{n}:

$$E_{\mathrm{n}} = \frac{1}{2} m_{\mathrm{n}} \left(\frac{d_{\mathrm{TOF}}}{T_{\mathrm{TOF}}} \right)^2 \tag{1}$$

where m_{n} is the neutron mass and $T_{\mathrm{TOF}} = T_{\mathrm{GS20\ signal}} - T_0$. Here $T_{\mathrm{GS20\ signal}}$ is the time of the ^{6}Li-doped GS20 detector trigger and T_0 is the time of the neutron interaction in plastic scintillator.

Choosing optimum dimensions of the plastic moderator is essential for maximizing the epithermal neutron flux incident on ^{6}Li-doped GS20 glass detector placed perpendicular to the source-moderator axis. This angle was chosen to avoid being in the straight line-of-sight of the source. As the source is embedded in a thick well of borated polyethylene and B_4C, the GS20 glass detector is shielded from most of the fast neutrons emitted. Only the plastic scintillator detects direct fast neutrons which get moderated via multiple elastic scattering interactions with the protons. A fraction of these fast neutrons end up in the epithermal range and out of those neutrons a very small number make it to the GS20 glass detector. The final numbers of epithermal neutrons detected in GS20 are determined by the cross section of neutron scattering in plastic and the solid angle covered by GS20 detector. Since the rate of detection of fast neutrons in plastic is much higher compared to the rate of detection of epithermal neutrons in GS20 detector, a correct correlation of an event in GS20 with the event in plastic scintillator for real coincidences requires a neutron detection rate comparable to the time-of-flight of the slowest neutron, which in this case is $\sim$ 32 μs. Based on these calculations, source rates of 10^5 neutrons/s and 10^4 neutrons/s were simulated. Ideally, these rates would ensure that very few subsequent neutrons are detected in the plastic scintillator within a window of 32 μs . However, detection of neutrons scattered from the surrounding materials can lead to false correlations and hence random coincidences. These events would then show as background counts in the time-of-flight spectrum. Therefore, it is essential to understand the role of source activity in reducing the background contributions. Another dominant source of background is the detection of on-axis thermal neutrons and off-axis epithermal neutrons arriving from the sides of the detector. Thermal neutrons were filtered out with a 3-mm thick Cd foil placed in front of the GS20 detector assembly. Cd has a large cross section for capturing thermal neutrons below 0.5 eV. The unwanted epithermals are removed by surrounding the GS20 detector with 2.5-cm thick B_4C and a collimator opening in the front. This kind of shielding also filters most of the thermals incident from the sides. To establish the feasibility of the proposed approach for doing NRTA measurements, simulations were performed to study in details the following three main aspects of the experiment,

- Optimum moderator dimensions
- Effects of source activity on real and false coincidences observed between the two detectors
- Spectral sensitivity for identifying NRTA attenuation lines in W and Ag targets

B. Moderator Dimensions

Independent and dedicated simulations were run to get the number of epithermal neutrons in GS20 detector with varying moderator dimensions. The geometry used for this simulation was identical to the proposed experimental setup shown in Fig. 1. A cylindrical plastic scintillator detector acting as an active moderator was placed at a distance of 5 cm from the neutron source. Fraction of epithermal neutrons detected by the GS20 detector for a 1"×1", 2"×2", 3"×3", 4"×4", 5"×5", 6"×6", 7"×7", 8"×8" and 9"×9" plastic scintillator are plotted as a function of moderator-detector diameter in Fig. 2.

Distance between the GS20 detector and moderator face was kept constant at 50 cm. Results show that the epithermal neutron flux increases with increasing moderator dimensions (both diameter and height of the cylinder were modified), saturates and then decreases. The initial increase in the fraction of epithermal neutrons reaching GS20 glass is because of more scattering of fast neutrons in the moderator. The fraction decreases after the optimum thickness because additional scattering results in the reduction of the neutron energies to below eV. The maximum epithermal fraction was obtained for a diameter between 15.2 cm to 20.3 cm. The following simulations were all done with an optimum moderator dimensions of 17.8 cm × 17.8 cm.

To understand the effect of moderation on the TOF resolution, simulation results were analysed for uncertainty in arrival time of epithermal neutrons at the face of the moderator. At 1 eV, a spread of 7 μs in the arrival time of neutrons for a 17.8-cm × 17.8-cm moderator was observed which reduces to 3 μs at 20 eV.

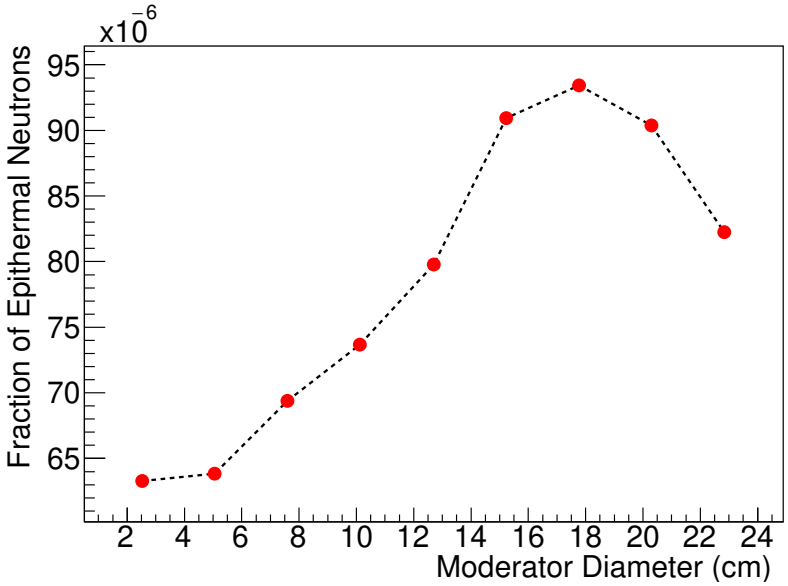

FIG. 2. Fraction of epithermal neutrons detected in GS20 glass detector as a function of moderator diameter. Time-of-Flight distance between front face of moderator and GS20 detector is kept constant at 50 cm for different dimensions of plastic scintillator acting as moderator in these simulation runs. A maximum flux of epithermal neutrons is obtained for 17.8-cm $\times$ 17.8-cm moderator, consequently chosen as the optimum dimensions.

C. Source Activity

Accurately reconstructing the neutron energy from measured TOF requires reducing the large backgrounds in the form of false coincidences between the plastic scintillator and ^{6}Li detector. One of the main sources of false coincidences are fast neutrons detected in plastic scintillator getting randomly correlated with an epithermal neutron in GS20 glass detector. Reducing the randomly correlated coincidences requires a detection of few neutrons in plastic scintillator within a window of 32 μs which is the time-of-flight of a 1 eV neutron across 50 cm distance. This constraint did not allow using a source activity of more than 10^5 neutrons/s. A neutron emission rate of 10^4 neutrons/s was also simulated for comparing the false coincidence levels in the transmission spectrum. The other contribution to background comes from direct fast neutron captures in GS20 glass. ^{6}Li has a resonance at 243 keV which enhances the cross section of capturing a fast neutron producing alphas and tritons similar to the epithermal/thermal capture reaction. The main contribution of borated polyethylene and B_4C layers surrounding the whole experimental setup shown in Fig.1 is to reduce the fast neutrons reaching the detector. Neutrons getting moderated by the borated polyethylene layer are expected to get absorbed by the B_4C layer. The front collimator geometry furthermore shields the neutron detector from moderated neutrons arriving off-axis. In Fig. 3, a 2-dimensional plot of TOF reconstructed energy vs true energy is presented for an open beam. No targets were placed in front of the detector assembly for open-beam simulations. Real coincidences follow a clear diagonal demonstrating the capability of this technique and setup in extracting the correct energy of incoming neutrons from the measured TOF. False coincidences for 10^4 neutrons/s do not interfere much with the actual signal and are concentrated at low energies as expected. The probability of falsely correlating a random event in plastic detector to an epithermal neutron in GS20 glass increases for long TOF values because of the chosen source activity. As the source emission rate increases false coincidences start showing up at higher energies (short TOF) too. A signal-to-noise ratio (SNR) defined as the ratio of real to false coincidences of 8 was obtained for a source activity of 10^4 neutrons/s . For comparison, a similar plot for 10^5 neutrons/s is also shown in Fig. 3 (b). A much lower SNR of 1 was observed for this case. Comparison of neutron transmission spectra through a 3.25-mm thick W target for 10^4 neutrons/s and 10^5 neutrons/s given in Fig. 4 shows that the attenuation dips corresponding to resonances at 4.15 eV, 7.7 eV and 18.84 eV are visible in both spectra giving confidence for future experiments. However,

enhanced noise level in 10^5 neutrons/s spectrum makes it a less favorable case. These plots consist of 10^9 particles simulated in total which corresponds to a measurement time of around 30 hours for 10^4 neutrons/s and 3 hours for 10^5 neutrons/s activity. Long measurement times is a limitation of this method. Development of efficient background subtraction analysis methods would enable using the 10^5 neutrons/s data, thereby reducing the measurements time quite significantly.

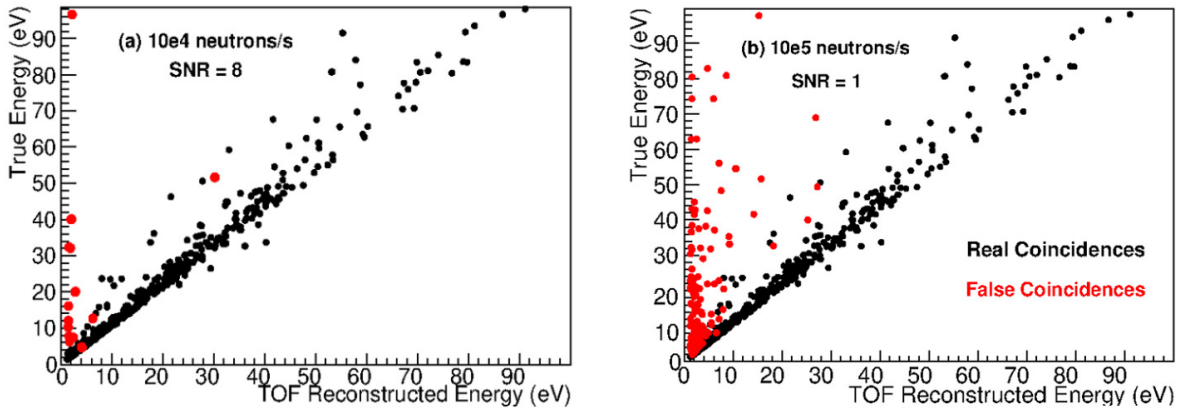

FIG. 3. (a) True energy vs TOF reconstructed energy for an open-beam run. Real coincidences between plastic and GS20 glass detectors are shown in black circles and false coincidences are in red. A source activity of 10^4 neutrons/s has a signal-to-noise (ratio of real to false coincidences) of 8. (b) With 10^5 neutrons/s much higher contamination from false coincidences is observed making the SNR = 1.

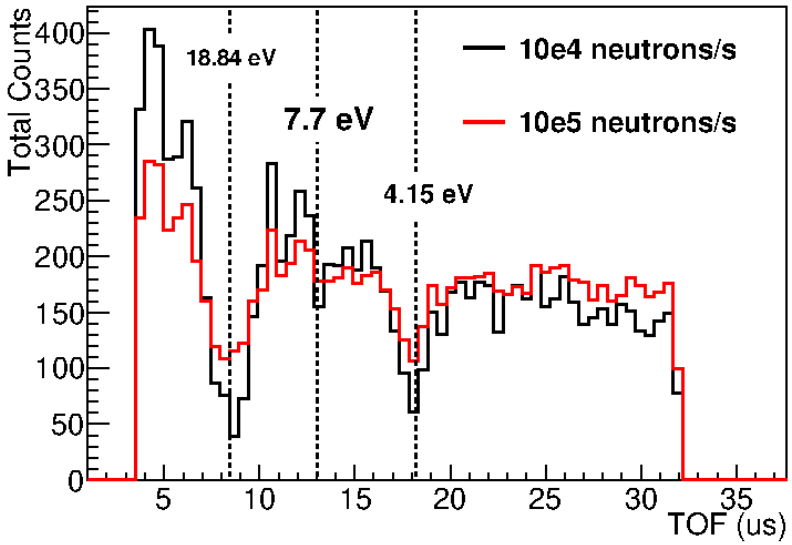

FIG. 4. (a) Neutron transmission for a W target with a source activity of 10^4 neutrons/s and 10^5 neutrons/s. Background levels due to false coincidences are enhanced in 10^5 neutrons/s case. The spectra are normalized for total counts observed in 10^4 neutrons/s to highlight the contrast in the observed ratio of attenuation-dips magnitude and the background.

In addition to neutrons with energy ranging from few keV to $\sim$ 11 MeV, AmBe source also emits 4.4-MeV gammas. For this work only neutrons were included in the simulations. Inclusion of gammas would further increase the number

of false coincidences in the transmission spectrum. If a liquid scintillator is used as the moderator instead of a plastic scintillator, pulse-shape discrimination can be exploited for separating out gamma contributions. This discussion is a part of future effort.

D. NRTA of W and Ag targets

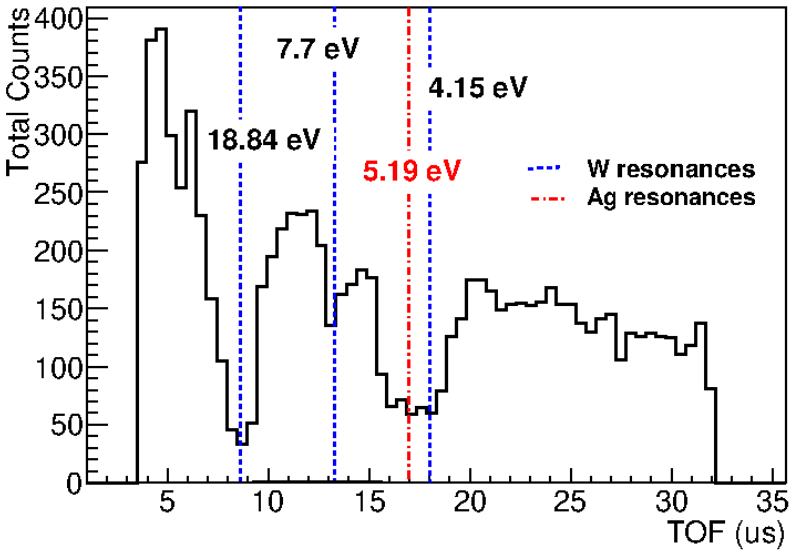

FIG. 5. Neutron transmission for a composite target of W and Ag. Better spectral resolution is needed to distinguish between 5.19-eV Ag resonance and 4.15-eV W resonance but a weak 7.7-eV line is well separated from the 4.15-eV strong W resonance. The source activity was 10^4 neutrons/s.

Determining the isotopic composition of composite targets demands a resolution good enough to unambiguously identify individual resonances. A simulated transmission spectrum with a multi-element target of W and Ag shows the ability of this technique to differentiate between closely lying resonance lines. Fig. 5 demonstrates that the resolution of this setup is sufficient to resolve the 4.19-eV and 7.7-eV resonances in W but not good enough to distinguish the former from the 5.19-eV resonance in Ag. As the spectral resolution is dominated by the spread in moderation time, it improves with increasing energy of neutrons. However, due to low statistically significant counts above E_n >20 eV, the TOF resolution could not be determined above that energy value. For nuclear security applications requiring identification of ^{235}U, better resolution is needed as the isotope has several weak and closely-spaced resonance lines. Longer TOF distances for improving the resolution would further increase the measurement times therefore are not considered here. Another solution could be to use a source emitting low-energy neutrons such as ^{252}Cf requiring thinner moderator for producing epithermal neutrons.

IV. CONCLUSION

In this work we have demonstrated the feasibility of performing isotopic identification with NRTA measurements using an AmBe source. The neutron transmission spectra for individual elements such as W and Ag had unique attenuation dips at resonance energies in the range of 1-20 eV. The simulation results showed that a compact and mobile NRTA setup could be built to do table-top experiments for material identification which would allow for

practical applications in the field of nuclear security and safeguards. An on-site analysis facility would limit the mobility of special nuclear material.

The technique and setup presented in this report however have few limitations. The constraint of using a low activity source to minimize the false coincidences between two TOF detectors results in long measurement times. Development of robust background estimation and subtraction algorithms should be explored to allow for higher source rates. Another limitation of this method is the spectral resolution which is dominated by the time spread of the epithermal neutrons resulting from the moderation. This time spread can be shortened by using a ^{252}Cf source. Maximum energy of emitted neutrons is $\sim$ 1 MeV thus the number of collisions with the $^{1}_{1}$H atom required to bring them down to $\sim$ eV energies are relatively less. Therefore, time spent by these neutrons in the moderator is less compared to the AmBe source giving a narrower time spread and a better TOF resolution. Future studies would concentrate on doing similar simulations with a ^{252}Cf source and validating the proof-of-concept with experiments.

V. ACKNOWLEDGEMENTS

This work was supported by Department of Energy Award No. DE-NA0003920, as part of the NNSA Consortium of Monitoring, Technology, and Verification (MTV). The authors would like to acknowledge the encouragement and advice of colleagues in MTV and the MIT Department of Nuclear Science and Engineering.

[1] D. L. Chichester and J. W. Sterbentz, Assessing the feasibility of using neutron resonance transmission analysis (NRTA) for assaying plutonium in spent fuel assemblies, Journal of Nuclear Materials Management (2012).

[2] M. A. Bourke, S. C. Vogel, S. L. Voit, K. J. Mcclellan, A. S. Losko, and A. Tremsin, *Non destructive examination of UN/U-Si fuel pellets using neutrons (preliminary assessment)*, Tech. Rep. (Los Alamos National Lab.(LANL), Los Alamos, NM (United States), 2016).

[3] P. Schillebeeckx, B. Becker, H. Harada, and S. Kopecky, Neutron resonance spectroscopy for the characterization of materials and objects, in *Supplement to Volume I/24* (Springer, 2015) pp. 10–66.

[4] C. Andreani, G. Gorini, and T. Materna, Novel neutron imaging techniques for cultural heritage objects, in *Neutron Imaging and Applications* (Springer, 2009) pp. 229–252.

[5] J. W. Sterbentz and D. L. Chichester, *Neutron Resonance Transmission Analysis (NRTA): A Nondestructive Assay Technique for the Next Generation Safeguards Initiative's Plutonium Assay Challenge*, Tech. Rep. (Idaho National Laboratory, 2010).

[6] A. Tremsin, S. Vogel, M. Mocko, M. Bourke, V. Yuan, R. Nelson, D. Brown, and W. Feller, Non-destructive studies of fuel pellets by neutron resonance absorption radiography and thermal neutron radiography, Journal of Nuclear Materials **440**, 633 (2013).

[7] G. Festa, E. P. Cippo, D. Di Martino, R. Cattaneo, R. Senesi, C. Andreani, E. Schooneveld, W. Kockelmann, N. Rhodes, A. Scherillo, P. Kudejova, K. Biro, K. Duzs, Z. Hajnal, and G. Gorini, Neutron resonance transmission imaging for 3D elemental mapping at the ISIS spallation neutron source, Journal of Analytical Atomic Spectrometry **30**, 745 (2015).

[8] H. Hasemi, M. Harada, T. Kai, T. Shinohara, M. Ooi, H. Sato, K. Kino, M. Segawa, T. Kamiyama, and Y. Kiyanagi, Evaluation of nuclide density by neutron resonance transmission at the noboru instrument in j-parc/mlf, Nuclear Instruments and Methods in Physics Research Section A: Accelerators, Spectrometers, Detectors and Associated Equipment **773**, 137 (2015).

[9] C. Paradela, J. Heyse, S. Kopecky, P. Schillebeeckx, H. Harada, F. Kitatani, M. Koizumi, and H. Tsuchiya, Neutron resonance analysis for nuclear safeguards and security applications, in *EPJ Web of Conferences*, Vol. 146 (EDP Sciences, 2017) p. 9002.

[10] F. Ma, S. Kopecky, G. Alaerts, H. Harada, J. Heyse, F. Kitatani, G. Noguere, C. Paradela, L. Šalamon, P. Schillebeeckx, H. Tsuchiya, and R. Wynants, Non-destructive analysis of samples with a complex geometry by NRTA, J. Anal. At. Spectrom. **35**, 478 (2020).

[11] G. Noguere, F. Cserpak, C. Ingelbrecht, A. Plompen, C. Quetel, and P. Schillebeeckx, Non-destructive analysis of materials by neutron resonance transmission, Nuclear Instruments and Methods in Physics Research Section A: Accelerators, Spectrometers, Detectors and Associated Equipment **575**, 476 (2007).

[12] A. Losko, S. Vogel, M. Bourke, A. Tremsin, A. Favalli, S. Voit, and K. McClellan, Energy-resolved neutron imaging for interrogation of nuclear materials, in *Advances in Nuclear Nonproliferation Technology and Policy Conference* (2016).

[13] Y. KUSUMAWATI, I. OZAWA, Y. MITSUYA, T. SHIBA, and M. UESAKA, X-band electron LINAC-based compact neutron source for nuclear debris on-site screening using short-distance neutron resonance transmission analysis, E-Journal of Advanced Maintenance **11**, 46 (2019).

[14] E. A. Klein, F. Naqvi, J. E. Bickus, H. Y. Lee, A. Danagoulian, and R. J. Goldston, Neutron-resonance transmission analysis with a compact deuterium-tritium neutron generator, Phys. Rev. Applied **15**, 054026 (2021).
[15] "grasshopper", https://github.com/ustajan/grasshopper (2019).
[16] International organization for standardization, neutron reference radiations for calibrating neutron measuring devices used for radiation protection purposes and for determining their response as a function of neutron energy,, Draft Standard ISO/DIS 8529 , 054026 (1986).